6

Coastal Upwelling and Other Processes Regulating Ecosystem Productivity and Fish Production in the Western Indian Ocean

Andrew Bakun, Claude Roy, and Salvador Lluch-Cota

Abstract

The seasonal intensity of wind-induced coastal upwelling in the western Indian Ocean is investigated. The upwelling off Northeast Somalia stands out as the dominant upwelling feature in the region, producing by far the strongest seasonal upwelling pulse that exists as a regular feature in any ocean on our planet. It is surmised that the productive pelagic fish habitat off Southwest India may owe its particularly favorable attributes to coastal trapped wave propagation originating in a region of very strong wind-driven offshore transport near the southern extremity of the Indian Subcontinent. Effects of relatively mild austral summer upwelling that occurs in certain coastal ecosystems of the southern hemisphere may be suppressed by the effects of intense onshore transport impacting these areas during the opposite (SW Monsoon) period. An explanation for the extreme paucity of fish landings, as well as for the unusually high production of oceanic (tuna) fisheries relative to coastal fisheries, is sought in the extremely dissipative nature of the physical systems of the region. In this respect, it appears that the Gulf of Aden and some areas within the Mozambique Channel could act as important retention areas and sources of "seed stock" for maintenance of the function and diversity of the larger regional biological ecosystems.

Introduction

The western Indian Ocean is the site of some of the most dynamically varying large marine ecosystems (LMEs) that exist on our planet. The Somali Current develops during the Southwest Monsoon to become the fastest open-ocean current in the world. The coastal upwelling that occurs along the Eastern Africa coast during the intensified phase of the Somali Current constitutes the most intense large-scale seasonal coastal upwelling system in the world. Other nearby regions are also strongly influenced by the annually reversing monsoon regime. This region is clearly unique in the world's oceans. However, in many ways, the region is also uniquely puzzling. For one thing, the coastal fish production seems positively minuscule for such a large area of ocean. The coastal fishery yield along the entire western boundary of the Indian Ocean, including the various island states of the western half of that ocean, represents far less than 1% of the global landings (1). Despite this, most fish stocks of the region are considered to be fully exploited or overexploited (1).

Moreover, in most LMEs of the world, the coastal fisheries production far outweighs the production from oceanic species such as tunas, generally constituting 90% to 95% of the total landings. But for the area of the southwestern Indian Ocean, the tonnage contributions of coastal and oceanic fisheries are approximately equal. The Indian Ocean continental shelf of Africa is relatively narrow, and this might provide some explanation for the low coastal landings. However, the disparity in continental shelf area compared with other ocean regions would appear to be far less drastic than would be necessary to adequately explain the anomalies in fish production.

Although the coastal fisheries are harvested mostly by the local countries, the more lucrative oceanic fisheries are harvested principally by distant water fishing fleets from Europe and eastern Asia. Even so, and despite the low coastal landings, fishing and its associated economic activities are often extremely important to local economies. In some southwestern Indian Ocean countries, fish are nearly the sole source of animal protein available to the local populations. Moreover, in a region faced with severe scarcities of foreign exchange, exports of fishery products represent vital sources of exchangeable earnings.

The Small Pelagics Puzzle

One particularly puzzling aspect of the region concerns the apparent low abundance of small coastal pelagic fishes. Fisheries on small pelagic fishes, such as anchovies and sardines and their tropical analogues (sardinellas, thread

herrings, etc.), are by far the most productive class of fisheries in the world, contributing nearly one-half of total global landings. However, in the southwestern Indian Ocean, the estimated catch of small pelagics is only about 27,000 metric tons, compared with the total catch of more than 500,000 metric tons (2). Thus, the region is notable both for its bounty of large pelagic oceanic fish and for its dearth of the customarily much more abundant small coastal pelagics.

Although small pelagics in most parts of the world are used mainly to produce fish meal for animal feeds, they are highly desirable traditional human food items in parts of Africa. For example, in recent years Nigeria and other West African countries have imported substantial quantities of frozen small pelagics from Europe and South America to be used for direct human consumption. Thus, there is potential for an international market for small pelagic fishes harvested in the southwestern Indian Ocean, if resource availability and economic factors were favorable. Thus, development of fisheries on stocks of small pelagics might conceivably form a basis for increased employment, food for the local population, and foreign exchange earnings in a region in need of all of these.

Be that as it may, conventional wisdom holds that small pelagics are, for some reason, not abundant in this region. For example, a number of acoustic surveys by the Norwegian fisheries research vessel *Fridtjof Nansen* during the decade of the 1980s did not locate the sorts of major fishable concentrations of small coastal pelagics that would suggest a potential for viable commercial industrial fisheries in the region (3). However, there does seem to be some possibility that significant concentrations of small pelagics might occur in waters too shallow for the large survey vessel to operate or that the surveys might have coincided with some seasonal or interannual minima in abundance. Ardill and Sanders (2) indicated the following potential yields of small coastal pelagic fish within the exclusive economic zones of various countries in the region: Mozambique (75,000 metric tons), Madagascar (50,000 metric tons), Tanzania (20,000 metric tons), Somalia (75,000 metric tons), Seychelles (115,000 metric tons), and Mauritius (20,000 metric tons).

In most marine ecosystems, the midlevel of the trophic system is dominated by a very small number of small plankton-feeding pelagic fish (or krill) species that attain very large biomass. This midlevel has been called the "wasp waist" of the ecosystem (4; J. Rice, personal communication) because of the constricted numbers of species compared with the much more speciose upper (larger predatory fishes, coelenterates, seabirds, marine mammals, etc.) and lower (planktonic) trophic levels. Modeling studies have shown that variability in the trophic dynamics of these ecosystems may be largely dominated by

variations in these midtrophic level wasp-waist populations (5). Typically, the populations of small pelagic planktivores vary radically in size, possibly in direct response to fluctuations in ocean conditions, and these variations may have major effects on the trophic levels above, which depend on the wasp-waist populations as their major food source and also on the trophic levels below which are fed upon by the variable, but massive, wasp-waist populations. Thus, if there are no substantial small pelagic wasp-waist components in the coastal ecosystems of the southwestern Indian Ocean, intriguing scientific questions arise as to how the trophic systems operate without them and why, in doing so, they operate so differently from most other LMEs of the world.

A Comparative Climatologic Approach

To attempt to shed some light on the above issues, we apply the comparative method, a methodology to which the LME framework appears to be particularly well suited (6). Mayr (7) called the comparative method and the better known experimental method "the two great methods of science." The comparative method is the method of choice whenever circumstances make it impractical to control experimental conditions. Mayr noted that the comparative method has been responsible for "nearly all the revolutionary advances in evolutionary biology" (an area of science where the time scales tend to preclude experimental controls). In the case of LMEs, the large spatial scales of the relevant processes, the lack of control of the ocean-atmosphere system, and the inability to maintain the integrity of an experimental volume of water without somehow artificially containing it generally combine to rule out realistic controlled experiments. The comparative approach is an available alternative.

Over the past two decades, a group of informative climatologic studies of various LME-scale fish reproductive habitats has been performed using a consistent set of methodologies (6,8–13). The basic data in these studies have been the maritime weather reports routinely logged by ships at sea and later assembled by national and international meteorologic agencies. Recently, a new global file of these data, called the Comprehensive Ocean-Atmosphere Data Set (COADS), has been collected, quality controlled, and put into common formats and units (14), and a convenient CD-ROM version of this data file, with extraction and summary software, has been developed by the National Oceanic and Atmospheric Administration/ORSTOM/ICLARM CEOS project (15). These data form the basis for the quantitative aspects of the comparative study presented here. Initially, we use them to inventory the wind-induced coastal upwelling systems of the western Indian Ocean.

Upwelling Systems of the Western Indian Ocean

It is clear that the major "classic" coastal upwelling systems of the world's oceans are primarily wind driven (16). In these areas, the stress that the wind exerts on the sea surface tends to be oriented such as to transport surface water away from the coast. The resulting loss of water next to the coast is compensated by upward movement of water to the surface from deeper layers. This *upwelling* of subsurface waters into the surface zone brings with it subsurface water properties, nearly always yielding cooler surface-water temperatures in the upwelling zone than in other nearby areas.

Most importantly, the upwelling brings influxes of dissolved plant nutrients from the subsurface nutrient pool into the illuminated surface layers. As a result, coastal upwelling regions represent some of the most productive regions of the world's oceans (17). They are characterized by massive populations of small pelagic fishes such as sardines, anchovies, or their tropical counterparts. For example, in the late 1960s, a single fish species, the anchoveta (*Engraulis ringens*), exploited by a single country, Peru, produced more total tonnage of fish than all other fish stocks exploited by all other countries of North and South America combined.

Here we adopt the same methods for indicating seasonal levels of upwelling intensity that were used in the group of studies cited in the previous section. Initially, charts of wind stress and sea temperatures (18–20) and satellite infrared temperature and chlorophyll pigment imagery were examined to select potential upwelling sites for more quantitative investigation (sites so selected are shown in Fig 6-1).

During the development of the COADS data set by NCAR, computations were made of the smoothed lower and upper median deviation around the smoothed mean on the basis of 2-degree aerial quadrangles and a monthly time step. These means and limits are used to create trimming bounds for the variables to screen out highly suspect data values. In this study, we choose to use only wind observations that are within a range defined by the monthly means plus or minus 3.5 times the SD.

For estimating the stress of the wind on the sea surface, we follow the procedures established by Bakun et al (11). An estimate of the stress is formed from each individual wind report according to

$$\tau = \rho C_D \mid \mathbf{v} \mid \mathbf{v}, \tag{1}$$

where τ represents the stress vector, ρ is the density of air (considered constant at 0.00122 g/cm^{-3}), C_D is an empirical drag coefficient (considered constant at

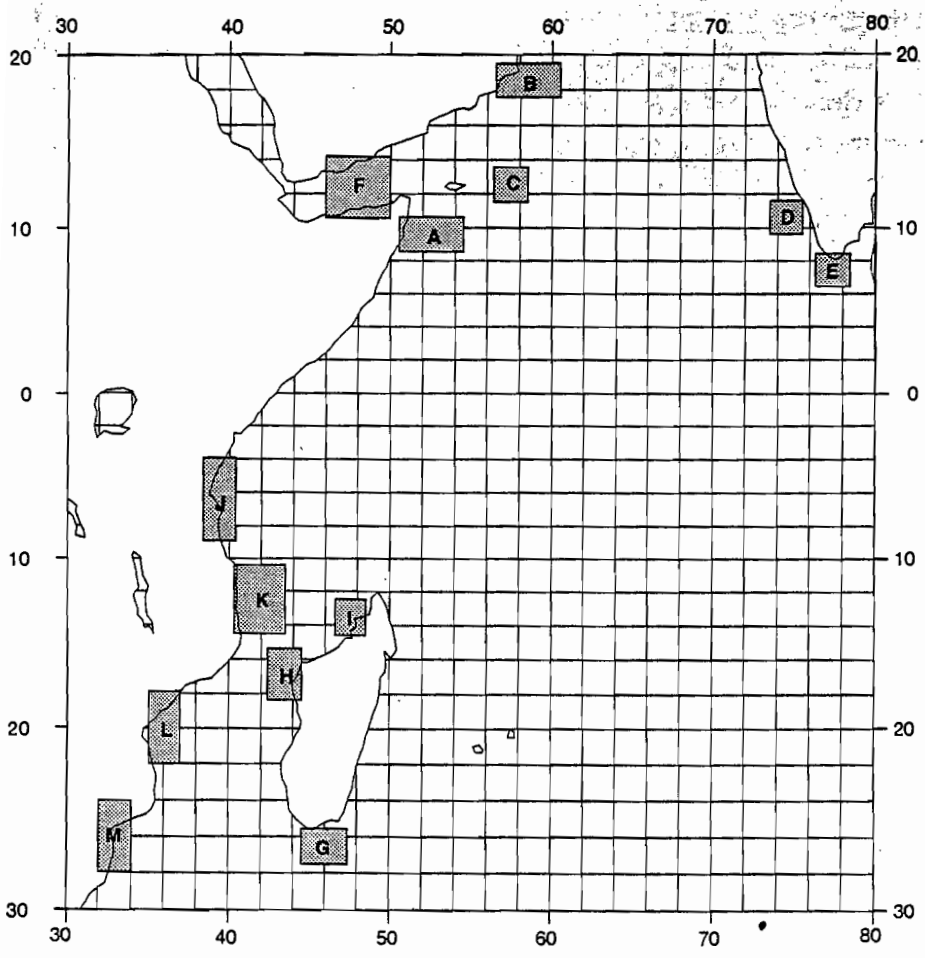

Figure 6-1. Geographic areas within which sea surface stress computations based on available surface wind reports have been pooled to produce long-term composite monthly coastal upwelling indices and "w^3" wind-induced turbulent mixing indices.

0.0013), $|\mathbf{v}|$ is the scalar wind speed, and $\mathbf{v}$ is the vector wind velocity. The estimates of the wind stress available within each of the areas indicated in Figure 6-1 for each calendar month were then averaged by component (vector averaged).

On the seasonal time scales being addressed, the drift of waters at the sea surface under the direct action of the wind stress is satisfactorily characterized by the simplified idealization known as Ekman transport (21). The net Ekman transport, **E**, integrated over the layer of some several tens of meters beneath the sea surface in which it occurs, is given by

$$E = k \times \frac{\tau}{f}, \quad (2)$$

where **k** is a unit vector directed vertically upward, $\times$ denotes the vector ("cross") product, τ is the wind stress vector, and f is the Coriolis parameter ($f = 2\,\omega \sin \phi$), where ω is the angular velocity of the earth's rotation and f is the latitude (negative degrees in the southern hemisphere). Net Ekman transport is thus directed perpendicularly to the right of the wind stress in the northern hemisphere and to the left of the wind stress in the southern hemisphere. Note that because the function of latitude is in the denominator of the expression, the Ekman transport corresponding to a given wind stress value increases very rapidly as distance to the equator becomes small.

Finally, the component of the Ekman transport directed perpendicularly offshore is resolved relative to the general coastal trend (on the size scale of the summary area). This represents a quantitative index (which we refer to as the coastal upwelling index [CUI]) by means of which levels of wind-driven upwelling intensity may be compared among different seasonal periods and among various upwelling sites.

Somali Coastal Upwelling

When these methods are applied to the western Indian Ocean, they yield striking confirmation of the remarkable strength of the coastal upwelling that occurs off the eastern coast of Somalia during the Southwest Monsoon. It appears to be by far the most intense seasonal-scale upwelling occurring in the world. The wind-induced upwelling component (Fig 6-2a) from June to August appears to be far stronger than occurs in the zones of most intense upwelling of the classic eastern ocean coastal upwelling zones (Fig 6-2, b, c, d, and e), in fact, six times stronger than the seasonal maximum near Lüderitz, Namibia (Fig 6-2d), which is considered to be the most intense of the eastern ocean upwelling systems (6).

The driving force behind this exceptional upwelling is a tropospheric wind current called the Findlater Jet. The Findlater Jet is the strongest low level atmospheric jet that exists as a regular feature anywhere in the world (22) and is a reaction to the steep surface atmospheric pressure gradient resulting from the extreme temperature contrast existing between the intensely heated Asian continental land surface and the cooler sea surface of the Indian Ocean. The jet extends northwestward from the coast of Somalia to cut diagonally across the Arabian Sea, where the shear zone along the northern side of the jet exerts intense cyclonic wind stress curl (18) on the sea surface which in

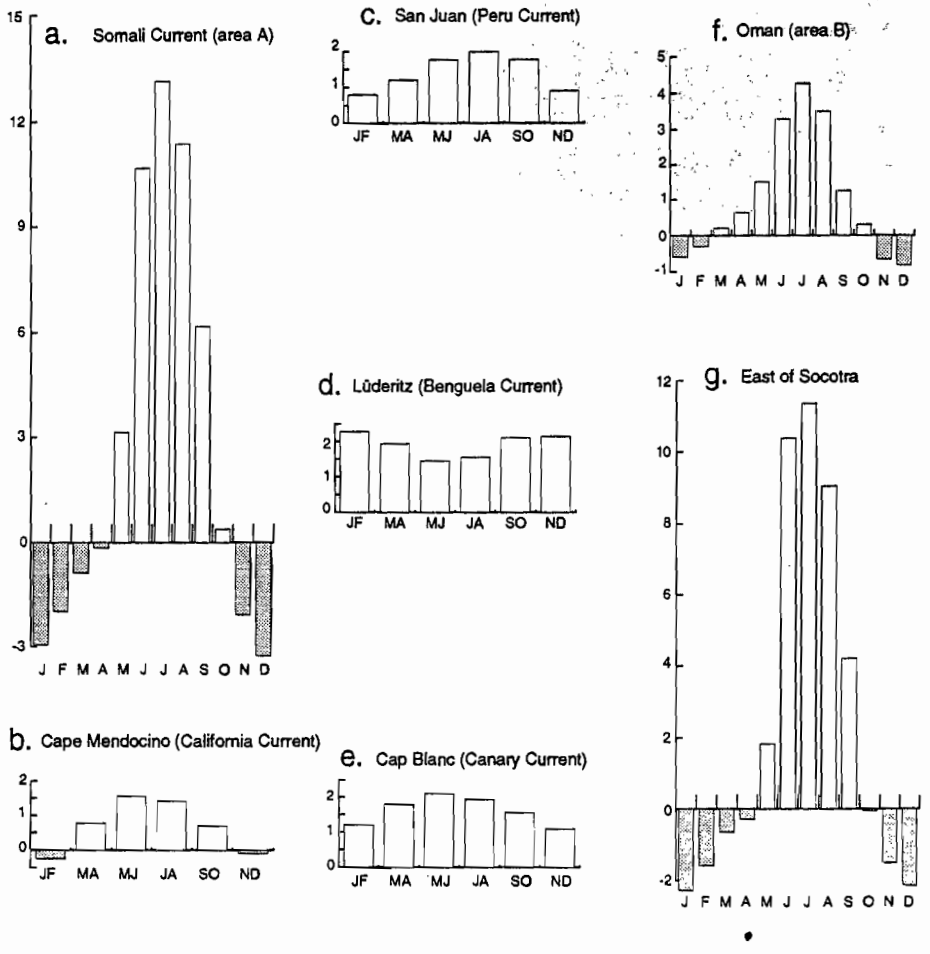

Figure 6-2. Long-term composite seasonal cycles of computed indices of wind-induced coastal upwelling in the upwelling maximum zones of various regions (T sec^{-1} m^{-1}): (a) off Somalia (see Fig 6-1, area A); (b) off Cape Mendicino, California (California Current); (c) off San Juan, Peru (Peru Current); (d) off Lüderitz, Namibia (Benguela Current); (e) off Cap Blanc, Mauritania (Canary Current); (f) off Oman (see Fig 6-1, area B); (g) at the stress maximum in the Findlater Jet east of Socotra (see Fig 6-1, area C).

turn drives an additional very energetic component of "open ocean upwelling" (23), extending from the African coast toward the far northern reaches of the Arabian Sea.

Upwelling off Oman

The extension of the Findlater Jet into the northern part of the Arabian Sea influences the coastal region of the Arabian Peninsula. Although the mean

position of axis of the jet is located some 500 km off the Omani coast, substantial wind levels associated with the feature do extend to the continental boundary where they produce substantial offshore Ekman transport (Fig 6-2f) and associated coastal upwelling. Although less than one-third the intensity level characterizing the core of the Somali coastal upwelling, this is still substantially larger in maximum seasonal magnitude than in any of the well-known eastern ocean upwelling areas (see Fig 6-2, b, c, d, and e).

Moreover, if one adds the contribution of the upwelling produced by the wind stress curl resulting from the shear zone on the near side of the Findlater Jet, one computes a total volume of upwelling, averaged over the zone extending 500 km seaward from the coast, that is nearly as large (Fig 6-2g) as that off the Somali coastal upwelling core itself (see Fig 6-2a). Accordingly, the picture emerges here of a 500-km wide zone of substantial upwelling intensity extending out into the Arabian Sea along its northwestern boundary. This zone stands out as a particularly striking feature of global-scale composite ocean color images from space (24), which clearly show the unusually wide bands of very high surface chlorophyll pigment concentration in the northwestern Arabian Sea.

Malabar Coast (Southwest India)

Upwelling off southwestern India, as indicated by rapid upward movement of isotherms (25), surface cooling (19), and depression of coastal sea level (26), occurs during the summer monsoon months from May to September (27). But rather than being alongshore and equatorward, as are the winds in most upwelling zones situated on eastern ocean boundaries, the summer monsoon winds off southwestern India blow almost directly onshore (19). However, Mathew (28) noted that near the coast there generally exists an equatorward component of wind stress (and therefore an offshore component of surface Ekman transport) throughout the year.

Our computations from the COADS data do indicate an average component of rather moderate offshore Ekman transport existing throughout the year (Fig 6-3a). But this does not explain very well the well-defined seasonality in the observed in situ evidence of active upwelling. Banse (27) and Longhurst and Wooster (26) suggest that these may result from upwarping of density surfaces in the clockwise gyre circulation that characterizes the Southwestern Monsoon in the Arabian Sea; that is, an effect of basin-wide wind forcing rather than local wind forcing.

However, if one examines the wind-driven offshore transport off Cape Cormoran, at the southern extremity of the Indian subcontinent, another

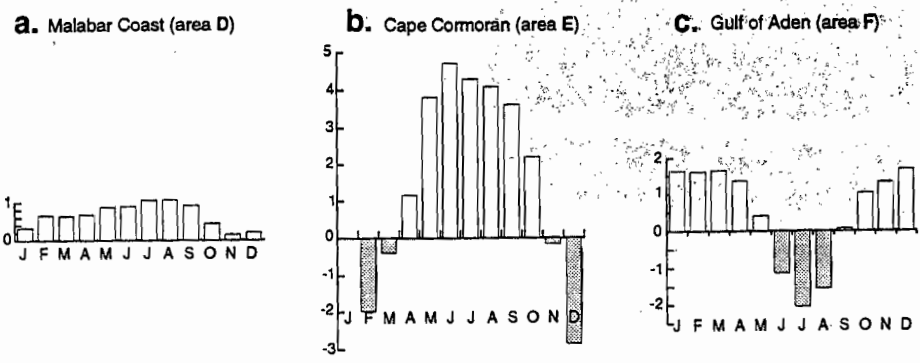

Figure 6-3. Long-term composite seasonal cycles of computed indices of wind-induced coastal upwelling (T sec^{-1} m^{-1}): (a) off the Malabar Coast (see Fig 6-1, area D); (b) off Cape Cormoran (see Fig 6-1, area E); (c) off the southern coast of the Gulf of Aden (see Fig 6-1, area F). Because the summary area spans the entire width of the Gulf, c applies equally well to the northern coast but in the opposite sense (i.e., negative values and downward bars indicate upwelling on the northern coast and positive values indicate coastal convergence).

explanation presents itself. Here, the strong westerly monsoon winds are tangential to the landmass and drive a very strong offshore Ekman transport (Fig 6-3b) that is in fact more than twice as large at peak seasonal intensity as in the strongest of the classic eastern ocean upwelling systems (see Fig 6-2, b, c, d, and e). This strong upwelling signal would tend to propagate northwestward along the Indian coast via the coastally trapped wave mechanism (a simple diagrammatic explanation of this mechanism is presented in Bakun [4]). Thus, coastal-trapped-wave propagation of the wind-forced upwelling signal off the southern extremity of the Indian landmass could account very well for the observed upwelling seasonality off the Malabar Coast. In such a case, when seeking an index of interannual variability in upwelling in this area, one should perhaps look at the coastal upwelling index off Cape Cormoran (see Fig 6-1, area E), which would depend on the general strength of the monsoon westerlies rather than that off the Malabar Coast itself (see Fig 6-1, area D), which would depend more on slight differences in the angle the westerlies might make with the large-scale coastline trend.

Coastal Upwelling Within the Gulf of Aden

Inside the Gulf of Aden, the wind is easterly (from the mouth toward the head of the Gulf) for most of the year (18). This produces offshore Ekman transport, favorable for coastal upwelling (Fig 6-3c), off the southern (Somalia) coast of the Gulf. However, during the Southwest Monsoon, the prevailing wind turns

around to blow from the southwest. Accordingly, during June, July, and August, the wind-driven Ekman transport is directed toward the southern coast and away from the northern coast. Consequently, during boreal summer, the coastal upwelling shifts to the northern coast of the Gulf, whereas the southern coast becomes a zone of coastal convergence.

Madagascar

The upwelling zones of the southern hemisphere areas of the western Indian Ocean are much less well known. Here, although we are able to compute a coastal upwelling index from surface wind data collected from logs of ships transiting the region, we have little corroboration in subsurface studies. Thus, our results are largely limited to describing the potential for upwelling that is inherent in the climatologic wind patterns. Thus, inferences as to the actual upwelling that may occur in response to these patterns should, at this point, be regarded as hypothetical.

Off the southern coast of the island of Madagascar, the easterly (westward) trade winds blow tangentially to the coast in an appropriate directional sense for producing offshore-directed Ekman transport. CUI computations (Fig 6-4a) confirm the existence of substantial offshore Ekman transport throughout the year, with a peak in late Austral winter. This is borne out by our examination of satellite sea temperature images, in which zones of lowered sea surface temperature often tend to be located adjacent to this stretch of coast. These zones at times take the form of plumelike shapes, which may extend from the southwestern "corner" of the island near Fort-Dauphin or from the vicinity of Cap Ste. Marie at the island's southernmost extremity.

Another zone of potential coastal upwelling off Madagascar is off the northwestern "corner" of the island, along the Mozambique Channel south of Cap St. André (see Fig 6-1, area H). Here, significant offshore-directed Ekman transport (Fig 6-4b) occurs during the months of northward-directed winds related to the Southwest Monsoon. However, when one examines satellite imagery for these months, the surface of the Mozambique Channel stands out as a particularly warm area, exhibiting little evidence of the coastal cooling that would signal substantial coastal upwelling. Thus, the actual upwelling situation in this location is unclear (at least to us).

Likewise, an area off northern Madagascar (see Fig 6-1, area I), just to the west of the northern extremity of the island, has appeared in satellite imagery as an area of substantial sea-surface chlorophyll pigment. However, our coastal upwelling index computations produced little indication of substantial persistent offshore Ekman transport (Fig 6-4c), although the data density in this area

was very low (accounting for the very "noisy" seasonal progression in Fig 6-4c). However, during the Southwest Monsoon, strong winds cross the northern peninsula of the island to blow directly offshore (18). It seems possible, at this low latitude location, that the Coriolis constraint may be weak enough for short, intense wind bursts to transport sufficient quantities of surface water

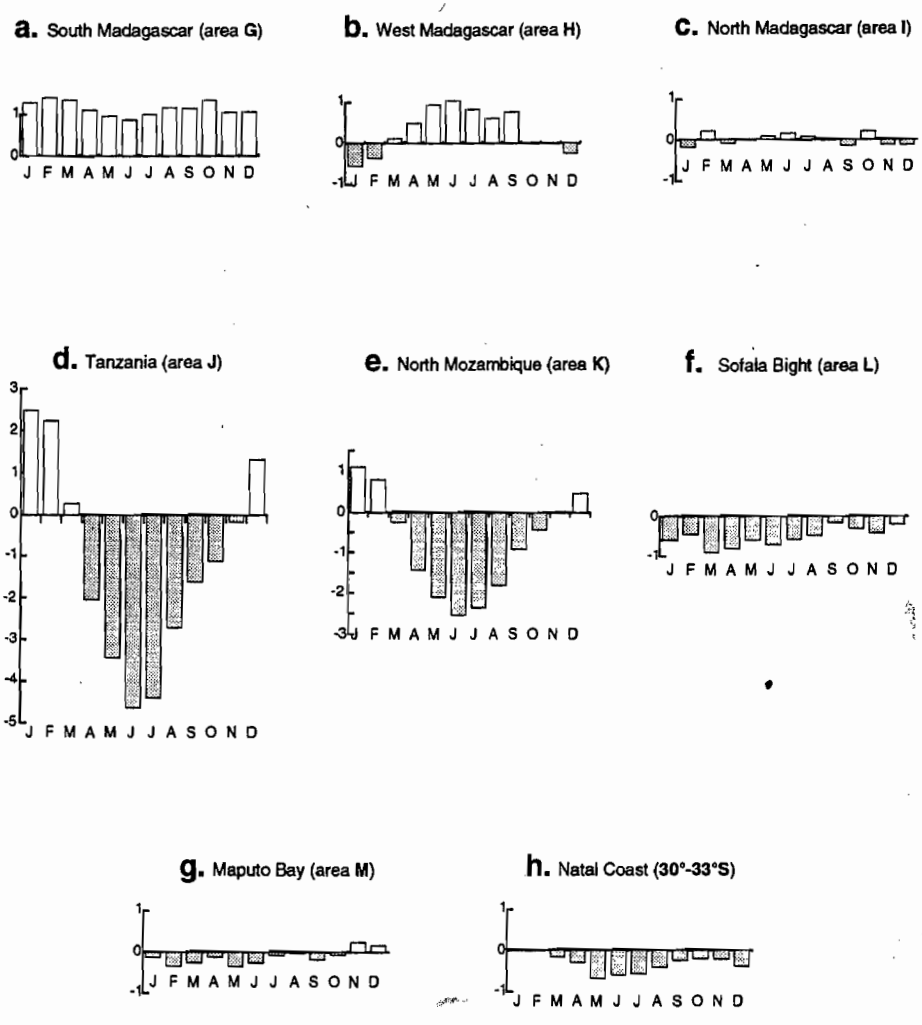

Figure 6-4. Long-term composite seasonal cycles of computed indices of wind-induced coastal upwelling (T sec^{-1} m^{-1}) at several locations on the coast of Madagascar: (a) off the southern coast (see Fig 6-1, area G); (b) near Cap St. André (see Fig 6-1, area H); (c) off the far northwestern coast (see Fig 6-1, area I); and at intervals along the African coast south of the equator; (d) off Tanzania (see Fig 6-1, area J); (e) off northern Mozambique (see Fig 6-1, area K); (f) off the Sofala Bank (see Fig 6-1, area L); (g) off Maputo Bay (see Fig 6-1, area M); (h) off the Natal coast (30 to 33°S).

directly downwind and offshore to cause significant upwelling at the coast. Such a phenomenon is observed at similar latitudes in the Gulfs of Tehuantepec and Papagayo off western Central America (29,30).

Tanzania and Northern Mozambique

During the Southwest Monsoon, the winds exert a generally northward stress over nearly the entire surface area of the western Indian Ocean. However, during the Northeast Monsoon, which occurs during the boreal winter half of the year, the wind pattern north of about 10°S latitude reverses to exert generally southward stress on the ocean surface. Along the African east coast, the area of reversal extends even further south, to about 15°S. This reversal turns the Ekman transport toward the coast and thereby "shuts off" the upwelling off Somalia (see Fig 6-2a), off Oman (see Fig 6-2f), and off southern India (see Fig 6-3b).

However, south of the equator, the Ekman transport is in the opposite direction with respect to the wind stress (90° to the left rather than to the right; see eq. 2). Thus, south of the equator, the Ekman transport responding to the southward wind stress of the Northeast Monsoon is directed offshore from the African coast (i.e., in the direction favorable to upwelling).

The wind stress intensity is roughly comparable and has quite similar seasonal cycles off the coast of Tanzania (see Fig 6-1, area J) and off northern Mozambique (see Fig 6-1, area K). However, because the magnitude of the Coriolis parameter (in the denominator of eq. 2) decreases rapidly in very low latitudes, the general level of Ekman transport off Tanzania (Fig 6-4d) is nearly twice as large as that off northern Mozambique (Fig 6-4e).

These are substantial CUI values, indicating a level of seasonal offshore Ekman transport certainly comparable, for example, with that in well-known coastal upwelling systems such as those off Cape Frio, in Southeastern Brazil (9) and off Portugal (31). Even so, characteristic sea-surface temperature patterns indicative of large-scale wind-induced coastal upwelling do not seem to be generally evident either off Tanzania or off northern Mozambique during the Northwest Monsoon period in either climatologic sea-temperature patterns, available nutrient distributions, or satellite imagery.

One possible explanation lies in the extreme seasonality of the region. The substantial offshore Ekman transports occurring in this part of the ocean during the Northeast Monsoon are, in fact, dwarfed by the more intense onshore Ekman transport of the opposite monsoonal period. This may so deepen the thermocline and nutricline near this coast during the Southwest Monsoon that upwelling due to the less intense offshore transport during the

Northeast Monsoon may not extend deep enough to entrain cooler nutrient-enriched thermocline waters. To phrase this in another way, the CUI computes an estimate of the upward mass transport through the bottom of the Ekman layer. If the Ekman layer does not extend to the vicinity of the bottom of the surface mixed layer, this upward transport may carry only mixed-layer waters, which have similar characteristics to those existing at the sea surface. In such a case, no spatial patterns indicative of upwelling would be apparent and no appreciable enriching effects of the upwelling would result. (Readers familiar with the El Niño phenomenon of the eastern Pacific Ocean may recognize an analogue in that El Niño tends to depress the thermocline next to the coast in a similar manner, either through a downwelling geophysical wave or, particularly off North America, through onshore Ekman transport produced via an atmospheric teleconnection. Consequently, the coastal upwelling, which tends to be even more vigorous than during non-El Niño conditions, does not produce the normal surface cooling and nutrient enrichment. Thus, one might say that the intense Southwest Monsoon forces the coastal ocean off Tanzania and northern Mozambique into a perpetual "El Niño-analogue" state, in which the upwelling during the opposite season is ineffective in modifying the surface properties.)

An additional contributing factor may be the location near the downstream end of the South Equatorial Current, which brings midocean tropical surface water toward this coastal region. Thus, the upwelling and downwelling mechanisms discussed above may operate within a larger scale background of warm, nutrient-impoverished upper ocean waters.

Southeastern Coast (Agulhas Current)

Along most of the eastern African coast south of the Zambesi River mouth (~19°S), the wind-driven Ekman transport field tends to have an onshore component throughout the year (Fig 6-4h). Thus, the sustained offshore Ekman transport that would drive conventional wind-induced coastal upwelling is largely lacking. Nevertheless, one frequently notices in satellite imagery various features suggestive of upwelling, usually associated with capes and seaward extensions of the continental shelf topography. One particular locus for such patterns is the vicinity of Cape St. Lucia (~28.5°S). Similar features, often suggesting plumelike structures being advected southward in the Agulhas Current flow, are also often evident off Pt. Zavera (~24.5°S) and various similar topographic protuberances of this coastline.

There are several mechanisms that might contribute to such topographically induced upwelling. In poleward-flowing western boundary currents such

as the Agulhas Current, frictional drag created by the current flowing against the shelf edge may lead, on a restricted local scale, to subgeostrophic flow (i.e., flow retarded to the extent that its Coriolis force no longer balances the ambient pressure force), a correspondingly unbalanced onshore-offshore pressure gradient, and resulting onshore transport in a bottom Ekman layer (32). The deeper waters moving shoreward over the continental shelf floor may then be mixed upward by turbulence generated by bottom friction. Additional mechanisms that may be involved include upwelling in small-scale eddies along the current edge (33), interactions between coastal trapped waves and bottom topography (34), and effects of interactions of internal tides with the shelf break and wind stress (35).

Southward of a point on the coast somewhat south of Durban, the waters over the continental shelf become substantially cooler than those further offshore. In large part, this is due simply to the offshore displacement of the high velocity core of the warm Agulhas Current flow that separates from the coast in this area. Moreover, the upward sea surface slope from the coast toward the higher standing, warmer, and somewhat less dense Agulhas Current surface water would tend to induce an inshore counterflow that could advect cooler, higher nutrient Atlantic surface waters northeastwardly along the coast. Even so, there are certain implications of local enrichment in this area that are consistent with local upwelling.

For example, the folder of ocean color imagery distributed by NSF/NASA (24) contains an impressive image (monthly composite for April 1979) of a large plume of water of high chlorophyll content at this location, having a shape definitely suggestive of advection in the Agulhas Current flow. The highest indicated chlorophyll concentrations are definitely located next to the coast and appear to spread from the upstream end of the plume. This indicates an upstream near-coastal source for the chlorophyll that, in turn, strongly suggests locally enhanced primary production due to upwelling or other local enrichment process, occurring along the zone of coast from about 32° to 34°S latitude.

At this point on the African coastline, one begins to encounter better studied regions. Along the "Cape south coast" it is known that the predominantly westerly wind flow is frequently broken, principally during summer by episodes of easterly winds (36). These events produce localized transient upwellings in the vicinity of major capes, etc. (37–42). As the continental shelf widens to form the Agulhas Bank at the Southern extremity of the African continent, other types of upwelling processes, including shelf-break upwelling and upwelling driven by cyclonic vorticity patterns in the wind and current flows (4,6,41) become increasingly important.

Reproductive Habitat Ecology

However, nutrient enrichment due to upwelling, and the resulting high rate of primary production, is evidently not the only determinant of fish stock productivity. Certainly, filter-feeding coastal pelagic fishes such as anchovies, sardines, and sardinellas are known to be inhabitants of particularly productive regions of the ocean, such as the eastern boundary upwelling systems. However, although high primary production may be a necessary condition for large stocks of these fishes to develop, it is apparently not a sufficient condition.

For example, one could certainly guess many regions of large coastal pelagic fish concentrations merely by looking at global-scale satellite ocean color images and choosing regions of particularly high chlorophyll pigment concentrations. But in some cases, one would be wrong, and one would certainly be mistaken on relative magnitudes. For example, on this basis, viewing the composite ocean color images distributed by NSF/NASA (24), one would guess the coastal pelagic fish populations off Peru to be smaller than those off California, equatorial Africa, and even Venezuela, but it is well known that coastal pelagic fish production off Peru is usually many times larger than the other three regions combined. Likewise, one might guess the very wide band of very chlorophyll-rich waters off the Arabian Peninsula, mentioned in the previous section, to be the habitat of particularly massive coastal pelagic fish populations. But, as discussed in the introduction, this is not the case.

The "Fundamental Triad"

Comparative studies of fish reproductive habitats have tended to identify a "fundamental triad" (4) of three major classes of processes that combine to yield favorable reproductive habitat for coastal pelagic fishes and also many other types of fishes:

1. *Enrichment* processes (upwelling, mixing, etc.);
2. *Concentration* processes (convergence, frontal formation, water column stability, ergoclines, etc.);
3. Processes favoring *retention* within (or drift toward) appropriate habitat.

The importance of enrichment processes is quite widely appreciated and is, of course, the reason for initiating this article with a survey of the regional upwelling systems.

Perhaps less widely appreciated is the importance of concentration processes. For very small organisms, such as fish larvae and other important com-

ponents of the planktonic food web, seawater represents quite a viscous fluid; major energy expenditures may be necessary just to move from food particle to food particle. Thus, large amounts of energy, needed for the rapid growth that is required for quick passage through the various size-related levels of intense predation that pervade the ocean environment, may be expended in feeding activity. Consequently, availability of processes whereby food particles are concentrated tends to be vital.

This is probably a major reason why various types of interfaces, or *ergoclines* (43), tend to be sites of enhanced biologic activity in the ocean. These interfaces tend either to maintain or to be maintained by mechanisms of concentration (4). Ocean fronts (Fig 6-5) are obvious examples. The importance of processes occurring in or near ocean fronts is suggested by the widespread attraction of fish and other marine animals to drifting objects. The actual convergent water motions associated with a front are probably too subtle to be directly sensed by pelagic organisms functioning in an environment devoid of fixed reference

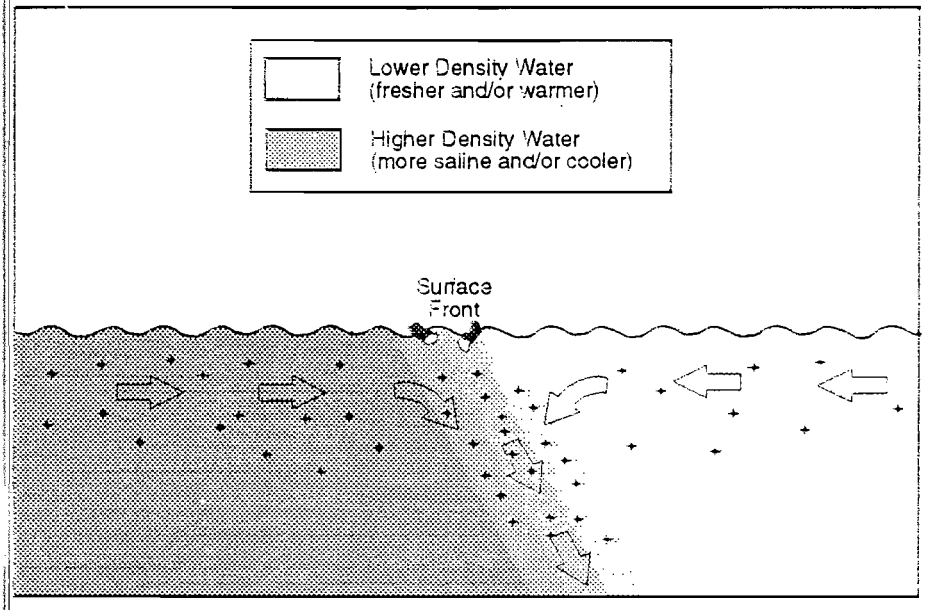

Figure 6-5. Schematic diagram of a front between waters of differing density. Arrows indicate density-driven flows associated with the front. "Particle" symbols indicate planktonic organisms capable of resisting vertical displacement. (Scales are distorted: vertical scale greatly expanded relative to horizontal; particles greatly magnified; surface waves not to scale, etc.) (Redrawn from Bakun A. The California Current, Benguela Current, and Southwestern Atlantic Shelf Ecosystems: a comparative approach to identifying factors regulating biomass yields. In: Sherman K, Alexander LM, Gold B, eds. Large Marine Ecosystems: Stress, Mitigation, and Sustainability. Washington, DC: AAAS, 1993:199–224.)

points. However, drifting objects tend to be carried into and to accumulate within frontal structures. An innate attraction to drifting objects serves to position the fish within the zones of enhanced biologic activity and correspondingly improved feeding conditions (4).

Conversely, turbulence is a dispersive process and so acts counter to concentration processes. Thus, intense turbulent mixing events have appeared to be detrimental to larval survival by disrupting local food concentrations (44–48). Moreover, although extremely small-scale turbulence may actually act like a concentration mechanism by increasing the encounter rate of small organisms with food particles (49), experimental evidence indicates that such

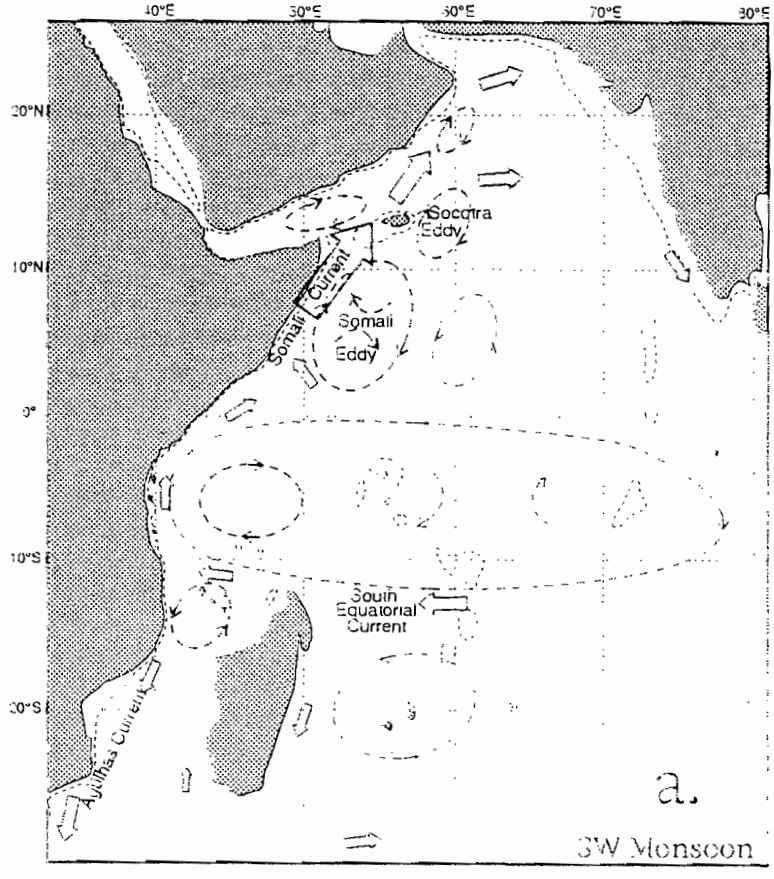

Figure 6-6. Schematic diagram of major features of seasonal surface circulation patterns in the western Indian Ocean. Dashed contours delineate the 200-m isopleth. Larger or smaller size of arrow symbols is intended to roughly indicate greater or lesser flow speed. (a) During the Southwest Monsoon.

an increase in encounter rate may be more than offset by a decreased ingestion rate, possibly due to difficulties in successful pursuit (50).

The third factor in the triad is retention. Life cycles of marine organisms tend to include at least one stage of passive larval drift. Thus, in a dispersive fluid medium, loss of early life stages from the population habitat may represent serious wastage of reproductive resources. Consequently, fish populations tend to spawn in locations and seasons that minimize such losses (12,51).

Surface Circulation in the Western Indian Ocean

As background for addressing the retention factor, we have constructed from various sources (19,20,22,52–54) the simplified schematic surface flow patterns characterizing the opposite monsoon seasons shown in Figure 6-6.

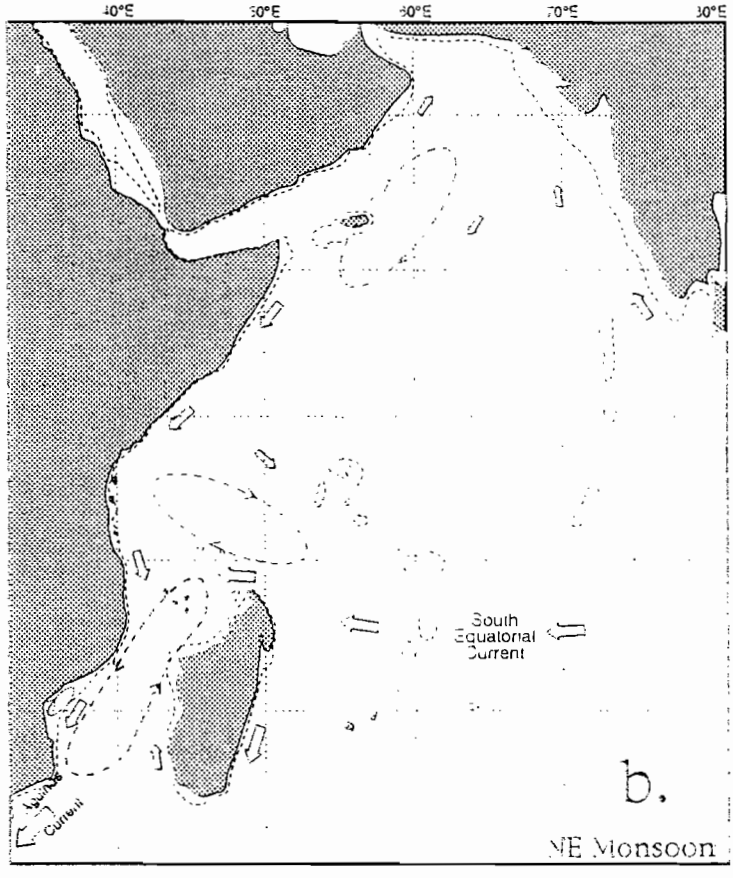

Figure 6-6. (continued) (b) During the Northeast Monsoon.

Several major features south of latitude 10°S appear to be quite persistent throughout the year. These include the South Equatorial Current, which flows westward through the region near 10 to 15°S latitude; the Agulhas Current, which flows southward toward the southern extremity of the African continent; southward flow along the east side of Madagascar; a tendency for a clockwise gyre pattern north of Madagascar; and a generally counterclockwise flow pattern within the Mozambique Channel.

North of the equator, the seasonal reversal of the Somali Current dominates the circulation pattern. There also generally seems to be a flow reversal off southwestern India. Thus, the flow pattern around the periphery of the Arabian Sea during boreal summer (Southwest Monsoon) is clockwise. However, during boreal winter (Northeast Monsoon), there is a counterclockwise tendency, with perhaps a segment of clockwise tendency in the very far north. The interior flows of the Arabian Sea during the Northeast Monsoon seem to be an irregular mixture of reversed superficial flows responding to the seasonal wind reversal and persisting remnants of deeper baroclinic flow features produced under the more intense summer monsoon conditions.

Reproductive Habitat for Coastal Pelagic Fishes

In summary, the western Indian Ocean evidently contains regions of particularly intense seasonal enrichment, both from upwelling and undoubtedly also from mixing due to the action of the intense monsoon winds on the sea surface and to the turbulence generated by the intense current shears and friction against the ocean bottom in shallow regions. However, mixing acts directly contrary to the second element of the triad, concentration. Also, the very strong current flows and wind-driven surface transport may act to defeat the third element, retention.

"Optimal Environmental Window"

A remarkably consistent finding in recent empirical studies of recruitment success of small coastal pelagic fishes is the existence of an "optimal environmental window" (55) with respect to wind intensity. When modern nonlinear empirical methods (56,57) have been applied to the historical time series of marine wind observations and recruitment estimates for the Peruvian anchoveta, the California sardine, the California anchovy, the Moroccan sardine, and the Senegalese and Ivorian sardinellas (55,58), the outcome has been the

consistently domed-shaped optimal environmental window result (Fig 6-7), where reproductive success tends to improve at intermediate wind speeds but to degrade when the characteristic wind intensities become either too high or too low. A study of the California sardine by Ware and Thomson (59), using slightly different methodologies, yielded a similar dome-shaped relationship.

Interpretation of the optimal environmental window in terms of the fundamental triad of enrichment, concentration, and retention appears to be straightforward. The control on the "low wind" side can be explained as a lack of sufficient enrichment of the trophic system by either wind-induced upwelling or mixing. The control on the "high wind" side could be a combination of the adverse impacts on the retention element of the triad due to the resulting excessive offshore transport and on the concentration element due to overly intense turbulent mixing that could disperse fine-scale concentrations of appropriately sized nutritious food particles (44–46), inhibit basic photosynthetic production by mixing phytoplankton cells beyond their "critical depth" (60,61), or impair a larva's ability to physically capture prey (50).

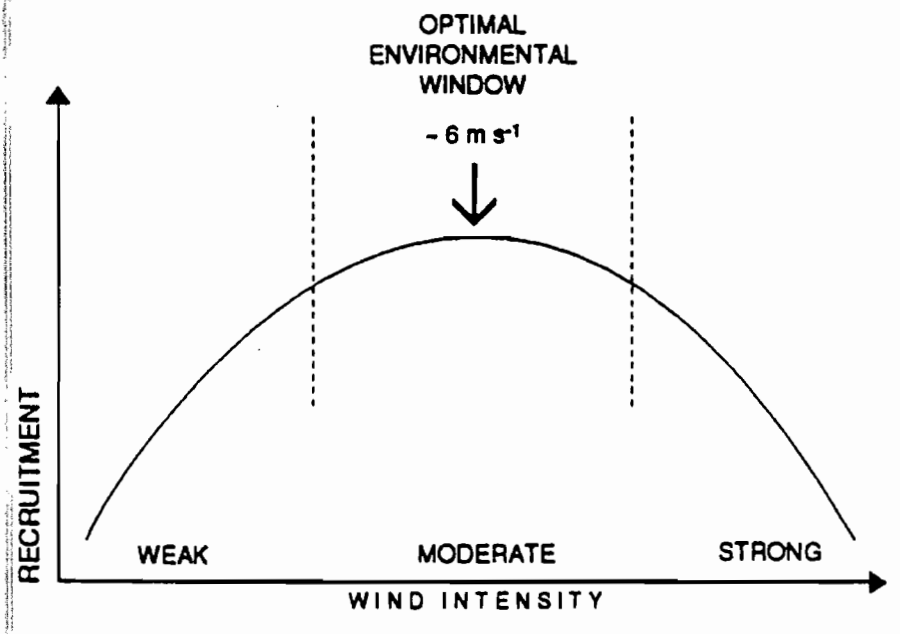

Figure 6-7. "Optimal environmental window" relationship between wind intensity and reproductive success in upwelling regions. (Redrawn from Cury P, Roy C. Optimal environmental window and pelagic fish recruitment success in upwelling areas. Can J Fish Aquat Sci 1989;46:670–680.)

Thus, the large populations of small pelagic fishes inhabiting coastal upwelling systems seem to be bound in a "midintensity level tradeoff" situation among the triad elements, which are in basic opposition in such upwelling systems (4). Although the fish may feed well as relatively strongly swimming, filter-feeding adults, because of the particularly high primary productivity of these systems, survival of their early stages may be severely limited by the other two triad elements.

In addition to the consistency in its general domed shape, the optimal environmental window result has been remarkably consistent in its indication of the ideal magnitude of seasonal wind conditions, repeatedly being found centered very near a mean seasonal wind value of 5 to 6 ms^{-1} (55,58). Thus, a mean seasonal wind value of 5 to 6 ms^{-1} would seem to be the point at which the detrimental effects of an increased general level of wind intensity on the other triad elements begins to predominate over the positive effects of increased enrichment. Moreover, from a study based on seasonal-geographic comparative studies rather than on time series analysis, Roy et al (62) pointed out that the observed spawning habits of small pelagic fish stocks off northwestern Africa fall into a pattern wherein the spatial locations of spawning grounds appear to particularly optimize larval retention, whereas the seasonal aspects of spawning appear to be tuned in a way that particularly limits exposure to turbulent mixing of the water column; the value of seasonal mean wind that was found to be limiting is again about 5 to 6 ms^{-1}.

Wind-Induced Turbulence Levels

The rate of input of turbulent kinetic energy to the ocean by the wind is roughly proportional to the third power, or "cube," of the wind speed (63). When climatologies of "wind speed cubed" have been compared with spawning habits of large populations of pelagic-spawning clupeoid fishes distributed around the world (9,10,31,64), a consistent pattern has tended to emerge such that the spawning habits are tuned seasonally and geographically in a way that minimizes the probability of encountering substantial wind mixing of the upper ocean. In fact, spawning habitats of these fishes are generally located where the seasonal average "w^3" index (or wind speed cubed) does not exceed 250 $m^3\ s^{-3}$ (6), except in cases where massive freshwater input or major overflow of one water mass by another may sufficiently oppose the breakdown of water column stability by wind action. Considering that the mean of the cubes of the actual observed wind speeds must be somewhat larger than the cube of the mean wind speed, this 250 $m^3\ s^{-3}$ value conforms remarkably well

to the 5 to 6 ms^{-1} limiting value that was identified in the optimal environmental window studies cited in the previous paragraph.

Somali Current

If one compares the characteristic values of the wind-cubed index in the various areas defined in Figure 6-1, it is clear that in the Somali Current areas, the values tend to greatly exceed the 250 $m^3 s^{-3}$ limit during the Southwest Monsoon upwelling season (Fig 6-8a). Thus, the concentration factor of the "triad" would seem to be very adverse, and the third component of the triad, retention, needs little additional discussion. Pelagic eggs and larvae of fish that spawn near the upwelling zones of the Somali Current are in for a 200- to 300-km/day "ride" toward an entirely different region of the Ocean. Thus, at the season when the enrichment factor is evidently highly favorable, the other two factors of the "triad" would seem to be extremely unfavorable along the western and northern coastlines of the open Arabian Sea. Although major semipermanent eddy systems such as the Somali eddy and Socotra Eddy (see Fig 6-6) may help to recirculate at least some larvae within the region, the system would seem to be an extremely dispersive one in which small organisms such as fish larvae may have difficulty finding sufficiently efficient feeding conditions to support the rapid growth needed for adequate survival rates.

Southwest India

However, as one follows the Somali Current flow around the periphery of the Arabian Sea, one arrives at the coast of India and an apparently more favorable possibility. Recall the hypothesis, developed earlier in this article, that the seasonal upwelling effects off the Malabar coast are a propagated response to the wind-driven offshore Ekman transport occurring some distance to the south off Cape Cormoran. In such a case, the fish are benefiting from an upwelling cycle that peaks in June (see Fig 6-3b). This propagating upwelling signal continues to be substantial from July to October. This also happens to be the period of the year when spawning activity of the Indian oil sardine, *Sardinella longiceps*, is most prevalent (26).

The turbulent mixing index near Cape Cormoran, where this upwelling would have its wind-generated origin, is substantial during most of this period, finally falling barely below the 250 $m^3 s^{-3}$ limit in October (Fig 6-8b). However, off the Malabar coast, where the resulting enrichment occurs, the turbulent mixing index has already approached this limit by August, falling well below it

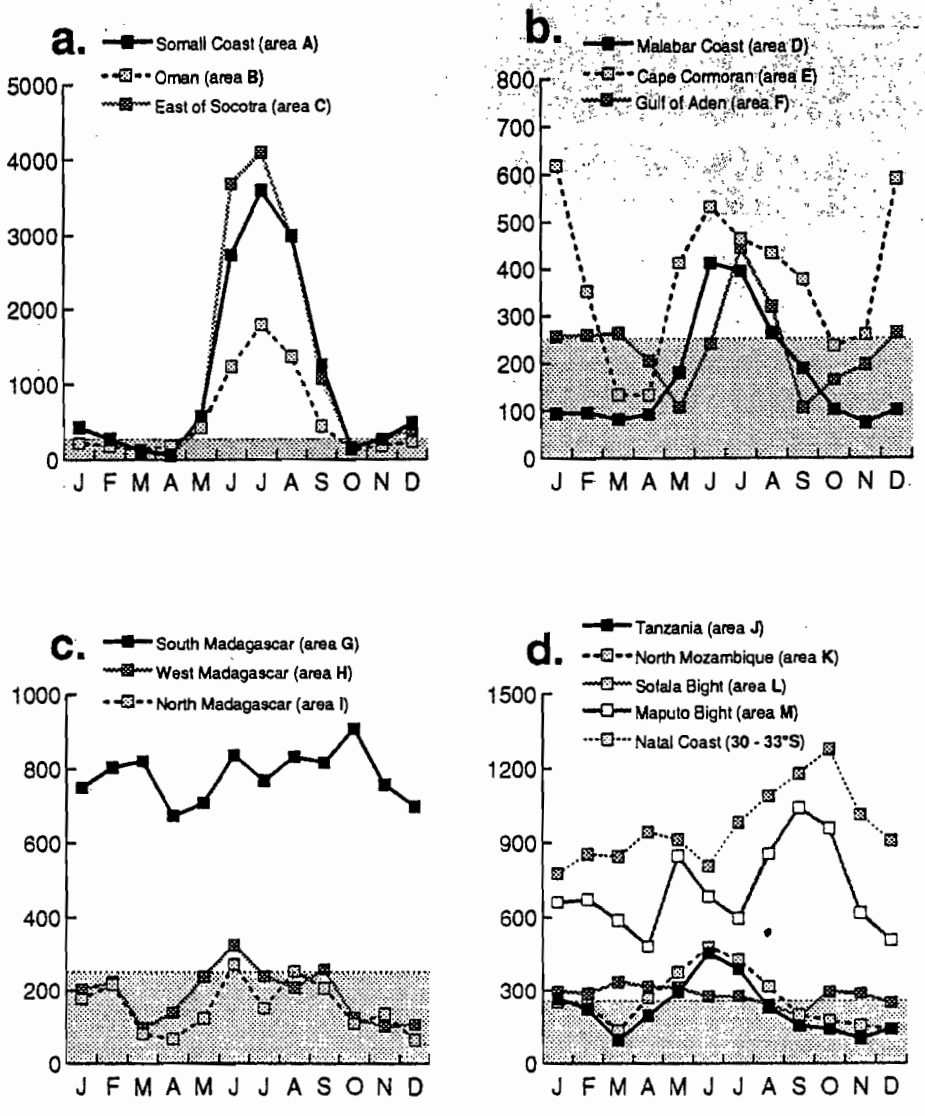

Figure 6-8. Seasonal cycles of "w^3" turbulent mixing indices for the various areas identified in Figure 6-1, produced as averages by month of the cube (third power) of wind speeds available in the historical files of maritime reports. Units are $m^3 s^{-3}$. Note that the scales vary among the four graphs. The area of each graph representing index values less than 250 $m^3 s^{-3}$, where comparative studies have identified favorable conditions for reproductive success of small coastal pelagic fishes, are shaded.

during the following months (actually being significantly above the limit only for the two months of June and July during the entire year).

By the time it has reached southwest India, the Somali Current flow is much less intense and has developed a more diffuse, meandering tendency (20) characteristic of eastern ocean coastal upwelling systems. Moreover, the local wind-driven offshore transport is fairly mild (see Fig 6-3a). Thus, the Indian oil sardine, which supports the western Indian Ocean's largest coastal pelagic fishery (annual landings fluctuating in the area of 200,000 metric tons in recent years), spawns in relatively mild offshore transport and wind-driven turbulence regimes of a tropical coastal upwelling system. Such spawning during the upwelling season is a recurrent pattern noted in other eastern ocean, low latitude pelagic fish stocks (62).

Gulf of Aden

Likewise, the southern coast of the Gulf of Aden would appear to offer another form of an acceptable triad configuration. Within the Gulf of Aden, the characteristic turbulent mixing index values (see Fig 6-8b) are at or below the limiting value during the entire year, except for the two-month July–August period. Substantial local coastal upwelling would appear to occur at the south coast throughout most of the remainder of the year (see Fig 6-3c). In addition, there is an apparent tendency for enclosed gyre circulations to form within the Gulf (see Fig 6-6) (20,54). Thus, a favorable set of enrichment, concentration, and retention processes would appear to characterize the south coast of the Gulf of Aden, except during the height of the Southwest Monsoon. During the Southwest Monsoon, there are winds favorable for coastal upwelling along the north coast of the Gulf (see Fig 6-3c), but this seems to be accompanied by a relatively high intensity of wind-induced turbulent mixing (see Fig 6-8b).

Madagascar

The coastal upwelling that may occur off southern Madagascar is apparently accompanied by quite high levels of wind-induced turbulent mixing (Fig 6-8c). Off western and northern Madagascar, the levels of turbulence generation would seem to be much lower (see Fig 6-8c). However, as discussed earlier, the upwelling that may occur in these areas would seem to be quite weak.

Tanzania, Mozambique, Natal

During the Northwest Monsoon upwelling season off Tanzania (see Fig 6-4d) and northern Mozambique (see Fig 6-4e), the index of wind-induced turbulent

nixing tends to be within the 250 $m^3 s^{-3}$ limit (Fig 6-8d). However, as noted earier, there is little indication of significant upwelling seen in surface-water properties. As discussed earlier, this might be due to the overwhelming dominance of he coastal convergence that occurs during the opposite monsoon season.

The area of coast that looks most promising as a reproductive habitat for small pelagic fishes is the large coastal bight off the Sofala Bank of Mozambique (see Fig 6-1, area L) where our computations indicate characteristic wind mixing values slightly exceeding the 250 $m^3 s^{-3}$ criterion. However, low data density in the region has caused us to use a summary area that extends well out of the bight where the exposure to the large-scale oceanic winds is greater than in the bight interior. Undoubtedly, there are areas deeper within the bight interior where the characteristic wind mixing values are much lower.

This coastal bight area has many of the characteristics of the most common type of sardine spawning habitat, being a coastal bight located downstream of a zone of wind-driven offshore transport of surface waters, where the coastal topography may serve to shelter the interior of the bight from strong wind-induced mixing and where an enclosed gyre circulation may help to retain pelagic eggs and larvae. Given that the offshore transport drives substantial upwelling-related nutrient enrichment (a fact that seems uncertain in this case; see above), there exists a spatial gap between the enrichment factor of the triad and concentration and the retention factors, which are linked through the large-scale alongshore advection. This spatial displacement, with organisms being advected with the flow experience as a temporal lag, allows the triad factors to be mutually supportive rather than in opposition (4,6).

In fact, the configuration of the "Sofala Bight" is very similar to that of the "Southeastern Brazilian Bight" (Fig 6-9) of eastern tropical South America, which has supported a major sardine (*Sardinella*) fishery for many years, with annual landings that initially grew rapidly to a peak of 228,000 metric tons in 1973, falling off thereafter to level of near 120,000 to 140,000 metric tons (65) that was maintained until 1986. Major differences include the fact that in the Brazilian case there is a definite local upwelling center (Cabo Frio-Cabo São Tome), where the surface characteristics of an upwelling zone are clearly apparent, just upstream (equatorward) of the bight. Even so, the seasonal cycles of chlorophyll look rather similar in the two different bight areas (see Fig 6-9). This leads one to at least suspect that a significant small pelagic fish component could find acceptable spawning habitat within the Sofala Bight, perhaps in waters too shallow for detection by large acoustic survey vessels.

Further south, in Maputo Bay and along the Natal coast, the characteristic wind mixing values rise to well above the 250 $m^3 s^{-3}$ limit (see Fig 6-8d) that appears to favor successful spawning of substantial coastal pelagic fish populations.

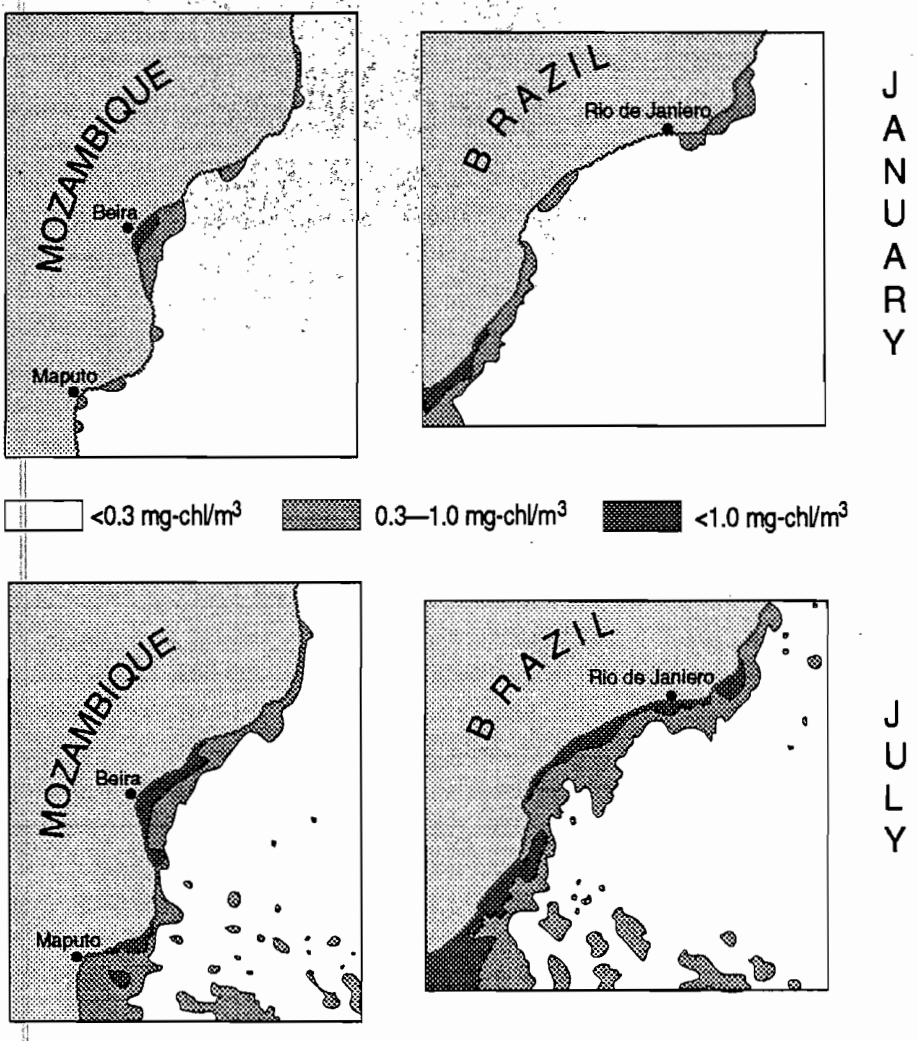

Figure 6-9. Multiyear composite mean monthly (January and July) distributions of sea surface chlorophyll pigment in the areas of the Sofala Bight of Mozambique and of the southeast Brazilian Bight produced from Coastal Zone Color Scanner satellite data. (For latitude reference, Rio de Janiero is situated at 23°S, Beira at 20°S, and Maputo at 26°S latitude.)

Habitat for Large Oceanic Pelagic Fishes

Although the reproductive problems for small coastal pelagic fish species have evidently contributed to the uncommonly low coastal fisheries production along the western edge of the Indian Ocean, fisheries on large oceanic pelagics (tunas, etc.) are substantial and lucrative. We may turn to the fundamental triad to offer some speculative reasons for this.

As indicated in the earlier sections, the coastal areas that should be most favorable with respect to the enrichment factor (e.g., the strong coastal upwelling zones of the Somali Current) are, due to the intense turbulent mixing and offshore transport that accompanies the upwelling process, extremely unfavorable with respect to the other two factors, concentration and retention. Thus, the high primary production is quickly swept offshore and broadly dispersed. Many types of small organisms that feed at the lowest trophic levels may have great difficulty in maintaining endemic populations against the incessant massive losses of individuals from the coastal area. Accordingly, much of the production may arrive offshore in a relatively unutilized state. This massive injection of unoxidized organic matter undoubtedly is one of the factors determining the very low dissolved oxygen concentrations found within and below the thermocline in the northern Arabian Sea (20,66).

The offshore areas of the western Indian Ocean are the habitat of widespread, highly dispersed populations of myctophids (lanternfish) and other small mesopelagic fishes. These are apparent beneficiaries of the offshore export of coastal production. These fishes have life-cycle strategies distinctly different from those of the coastal pelagics. They are diffusely distributed in less productive environments, evidently trading off lower growth rates for relatively mild predation rates, not expending energy in horizontal migration or in holding geographic position but rather relying on vertical migration within the vertically variable horizontal flow structure to avoid being swept en masse out of an ocean area, and relying on the food concentration mechanisms inherent to various interfaces (e.g., strong thermocline gradients, the sea surface, frontal structures, etc. [4]) to yield adequate feeding efficiency to support their comparatively "low-energy" life style. These small fishes, as well as invertebrate organisms using similar strategies, apparently are opportune prey for large pelagic predator fishes such as tunas, which are able to use the hydrodynamic advantages of their large size to efficiently cruise and feed along these interfaces.

Tuna, however, unlike mesopelagic fishes, use distinctly "high-energy" strategies at all life-cycle stages. Thus, tuna also may require their special variants of the fundamental triad to provide sufficiently rich food concentrations to support the voracious feeding and rapid growth of their early stages. Bakun (4) presented examples of how such triad arrangements might function in the spawning grounds of the Pacific albacore and the Atlantic bluefin tuna populations. Here we adapt aspects of those scenarios to the situation of the western Indian Ocean.

The locations of the maxima in the mean wind stress patterns during the opposite monsoon seasons are diagrammed in Figure 6-10. A persistent maxi-

mum in the sea-surface wind-stress field marks the demarcation between a closely linked "couple" of adjacent areas of divergence and convergence in the surface Ekman transport field (Fig 6-11). On the left side (when facing downwind) in the northern hemisphere and on the right side in the southern hemisphere, the Ekman transport is directed toward the line of maximum stress and increases in magnitude as distance from the line diminishes. Thus, the Ekman transport field is diverging as it approaches the line of maximum stress. As the water carried in the Ekman transport field crosses the line of maximum stress, the Ekman transport begins to steadily lessen in magnitude, and so the water is converging on that side.

The result is upwelling and corresponding enrichment on one side of the wind stress maximum and convergence, downwelling, and surface frontal formation on the other—in sum, a very closely linked coupling of the enrichment and concentration elements of the triad. We have discussed the rapid intensification of the Ekman transport field as the equator is approached. In near equatorial regions, there can be very intense Ekman divergence and convergence even at rather low wind intensity. Consequently, this enrichment-concentration couple acts in the absence of a correspondingly intense level of wind mixing that would tend to disperse concentrated food patches.

An additional coupled enrichment-concentration process may also operate in such a situation. The respective zones of divergence and upwelling and of convergence and downwelling overlie corresponding zones of doming and of downwarping of the subsurface density structure. Because of the resulting inclination of the density structure, surface geostrophic current jets often underlie strong wind stress maxima (compare Figs 6-6 and 6-10). These jets tend to produce eddy vortex action due to lateral friction. The dynamic processes involved in frictional formation of cyclonic vortices (counterclockwise in the northern hemisphere and clockwise in the southern hemisphere) result in upwelling (enrichment) in the cores of the vortices (Fig 6-12). Vortices rotating in the opposite sense produce convergence (i.e., a mechanism for concentration of organisms able to resist sinking with the slow downwelling within the eddy core). Moreover, the incremental deceleration of the larger scale flow by this frictional action represented by these vortices has the effect of reducing the Coriolis force that acts to maintain the sea-surface slope transverse to the current. This reduction in Coriolis force allows the higher standing, lighter waters to move down the slope to encroach on and mix with the heavier waters, forming a mixed water mass of greater density that flows under the lighter upslope surface water. This sinking motion between surface waters of different densities acts to produce a surface frontal zone and the associated concentration mechanism displayed in Figure 6-5.

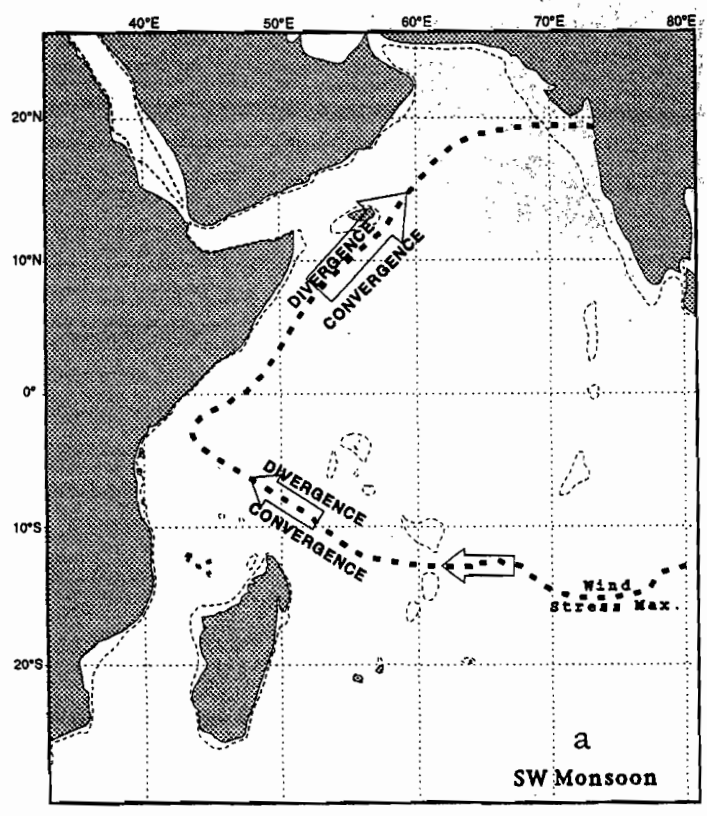

Figure 6-10. Mean positions of seasonal wind stress maxima in the western Indian Ocean (abstracted from the charts of Hastenrath and Lamb [18]): (a) during the Southwest Monsoon.

So one might construct a mental picture of cyclonic eddies in the vicinity of a strong current jet taking the form of moving "nutrient fountains" continuously injecting dissolved plant nutrients into the photosynthetic layers. Outside the cyclonic eddies, the zone of ocean in which the eddies are imbedded is generally convergent (due to the frictional breakdown of geostrophy and to anticyclonic eddy action). Here, a density-driven subflow, transverse to the flow of the current jet, acts to carry the enriched surface waters and their entrained planktonic food web toward convergent ocean fronts wherein the entrained organisms are concentrated (see Fig 6-5). This enrichment-concentration couple in turn operates within a wind-driven Ekman transport field in which surface water is being carried, again transversely to the flow of the current jet, from an area of Ekman divergence on one side of the wind stress maximum to an area of convergence on the other side (and, by the way, moving from the side of the underlying current jet where cyclonic eddies

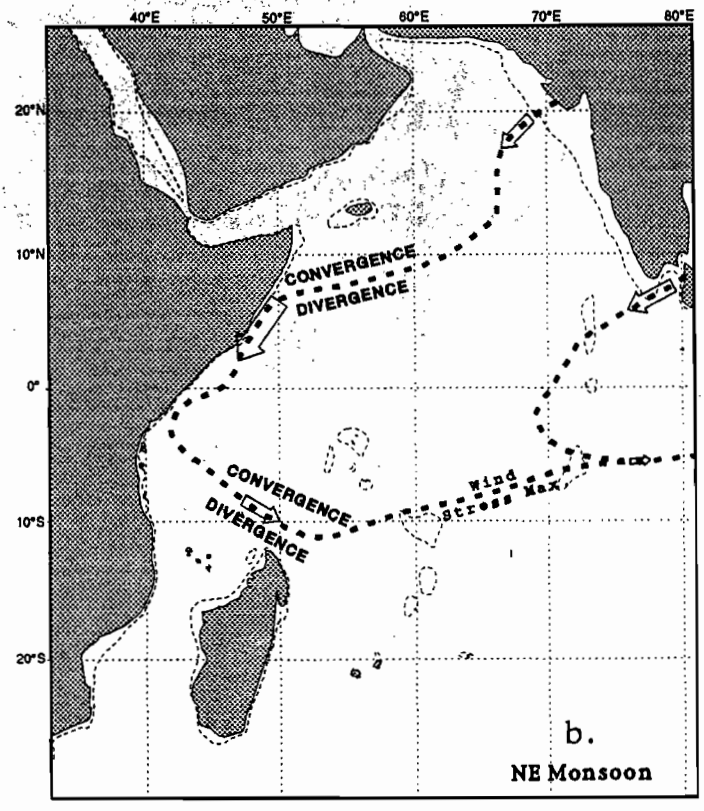

Figure 6-10. (continued) (b) During the Northeast Monsoon.

should predominate toward the side where convergent anticyclonic eddies should predominate). Thus, we have two nested, mutually supportive sets of coupled processes of initial enrichment and subsequent concentration, one set directly driven by the wind and the other by the underlying geostrophic current jet.

Thus, from the point of view of physical enrichment and concentration mechanisms, this would seem to be quite an advantageous situation in which weak-swimming early life stages have an elevated probability of being carried to and collected in zones of concentrated food distributions, where they may experience the accelerated growth rates needed to survive in substantial numbers through the numerous levels of size-dependent predation existing in marine ecosystems. In addition, young tuna seem to have their nursery habitat very much to themselves. Populations of fishes that might potentially prey on early life stages of tuna or have early stages that might in some way compete with early life stages of tuna are relatively lacking. Under such circumstances,

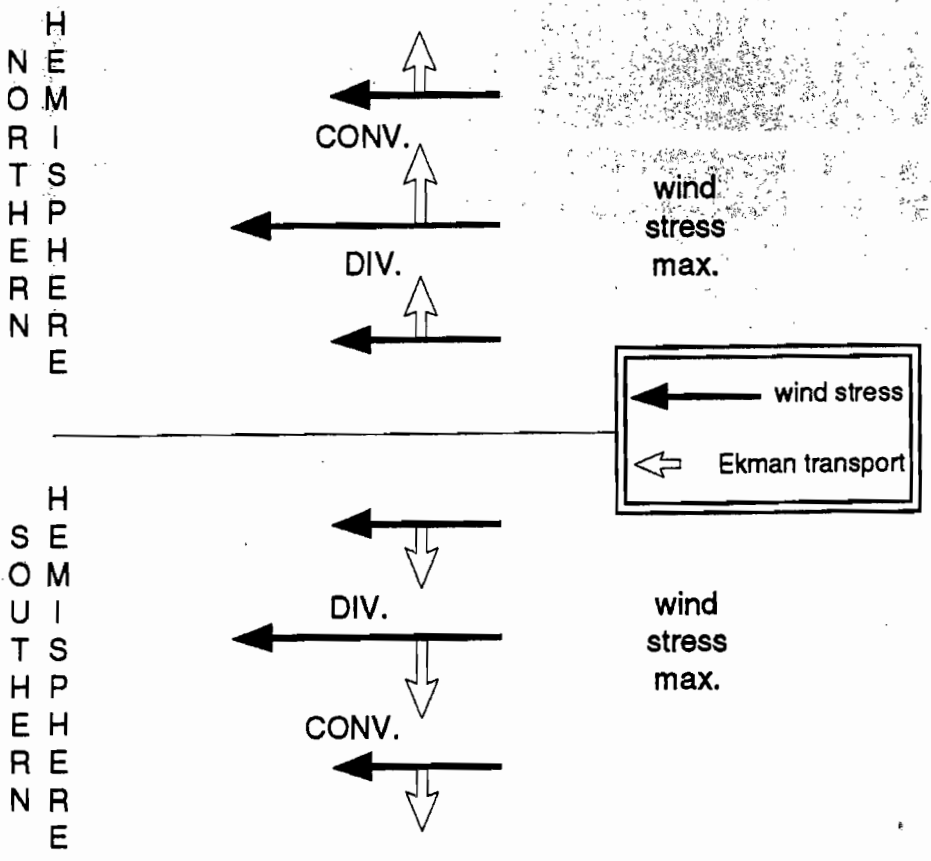

Figure 6-11. Diagram of zones of Ekman convergence and divergence on either side of a wind stress maximum. Relative magnitudes are indicated by differences in lengths of the vector symbols. (Reproduced by permission from Bakun A. Patterns in the ocean: ocean processes and marine population dynamics. San Diego, CA: University of California Sea Grant, in cooperation with Centro de Investigaciones Biológicas de Noroeste, La Paz, Baja California Sur, Mexico, 1996.)

where other types of prey fishes may be relatively absent, young tuna effectively may build their own trophic pyramid, with faster growing individuals cannibalizing smaller ones. In this way, surviving tuna larvae are able to gain access to the trophic energy gathered by much larger numbers of less fortunate members of the same cohort.

A major reason that other types of fish are relatively absent in the tuna nursery grounds is that in such an area of strong current jets, they may have great difficulties with the third element of the triad, population retention. Tuna grow to very large size and moreover take particularly efficient advantage of size-related hydrodynamic advantages. Accordingly, tuna are largely able to

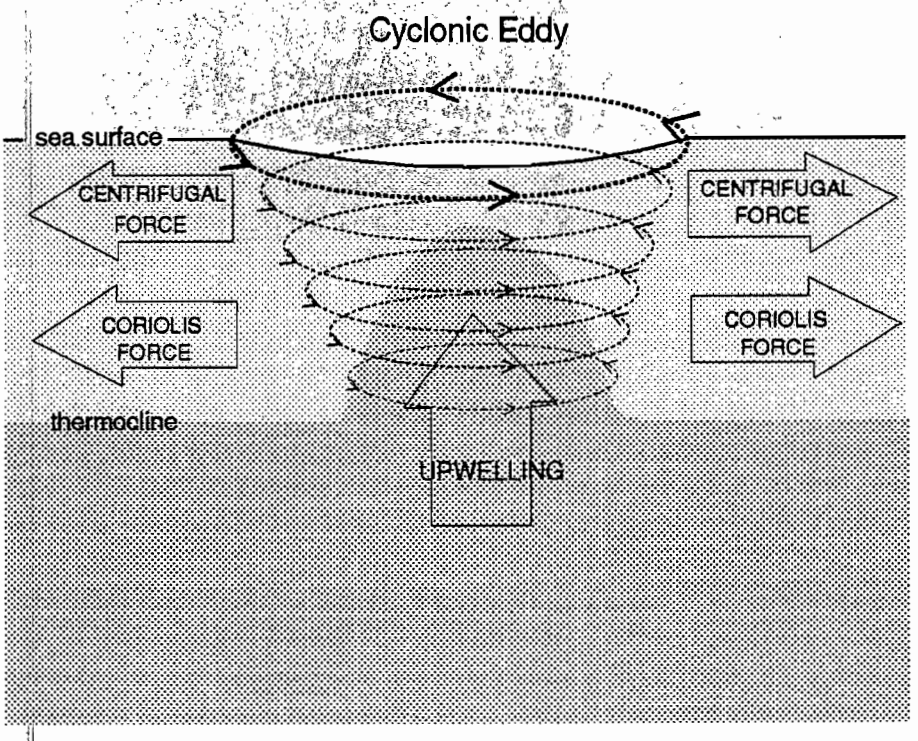

Figure 6-12. Upwelling occurring in a cyclonic eddy. Centrifugal and Coriolis forces due to the water motions are directed outward from the vortex center. In equilibrium (quasi-geostrophic balance), these are counteracted by inwardly directed pressure forces due to upwelling of deeper waters of greater density within the vortex core. (Reproduced by permission from Bakun A. Patterns in the ocean: ocean processes and marine population dynamics. San Diego, CA: University of California Sea Grant, in cooperation with Centro de Investigaciones Biológicas de Noroeste, La Paz, Baja California Sur, Mexico, 1996.)

solve their population retention needs by shear swimming power of the adults. In addition, tuna have migratory behaviors that make use of large scale current flows (67). Thus, it might be said that the population retention area (51) of a tuna species might have dimensions approaching those of the ocean basin itself. Smaller less migrationally capable fishes, such as might be important predators or competitors in other regions of particularly favorable combinations of the triad elements, would tend to be precluded from the tuna nursery areas by their inability to solve element three of the triad (4).

The smaller fish and invertebrate species that do manage to inhabit the tuna nursery areas must generally be strong vertical migrators to counter advective removal. This makes them available for predation by large adult tunas. Thus, these species may serve the function of carrying the production of the upper

ayers to the deeper layers inhabited by the large tuna. Young tuna stages, on he other hand, are able to rise to the surface layer where, having larger gill urface to body volume ratios than older, larger individuals, they are able to cquire adequate oxygen to meet metabolic needs in warmer surface waters. Surface area tends to vary as the second power of body length, whereas body olume, and thus body mass, varies as the third power of body length. Thus, urface-to-volume ratios decrease with increasing body length and so larger ish have greater difficulty acquiring adequate oxygen than smaller fish having he same general body form [68]. And because they are freed from the necessity or vertical migration by their avoidance of the requirement for local retention, hey can remain relatively separated by depth level from cannibalistic predation by the parental stocks of larger adults [4].)

Because the northern "core" lines of maximum wind stress (shown crossing the Arabian Sea in Fig 6-10) overlie extremely low dissolved oxygen concentrations within the thermocline of the ocean, these northern zones would appear to be less favorable spawning grounds for the large tuna species (yellowfin, *Thunnus albacares*; bigeye, *T. obesus*; and albacore, *T. alalunga*) than for the much smaller skipjack (*Katsuwonus pelamis*) that may be better able to meet adult metabolic oxygen needs in warm ocean surface waters (66,68). Consequently, the southern hemisphere maximum wind stress lines (see Fig 6-10) may delineate the better reproductive areas for the large tuna species, particularly the more temperate bigeye and albacore.

In summary, several environmental factors—the rapid export and dispersion of incompletely used production from the near-coastal ocean, the strong monsoonal wind circulations, and the associated prevalence of strong current jets—may underlie a more complex set of ecologic processes affecting trophic enrichment, concentration of food distributions, and advection of weakly swimming organisms. These processes may combine to shift the ecologic balance of the oceanic region of the tropical western Indian Ocean toward the unique, highly evolved life-cycle strategies of tunas to a sufficient degree to account for the extraordinary predominance of this species group in the fishery landings of the region.

Somali Current LME

We have presented certain quantitative data in the form of summaries of maritime wind observations formulated as indices of wind-induced coastal upwelling (see Figs 6-2 to 6-5) and rate of addition of turbulent mixing energy to the ocean by the wind (see Fig 6-8). Seasonal cycles of the magnitudes of

these indices have been compared among different locations within the southwestern Indian Ocean region and with comparable indices available from some better known LMEs. The comparisons, combined with other available knowledge, have allowed us to propose some hypothetical rationalizations for some of the unique aspects of this region.

We may consider whether these (admittedly speculative) rationalizations may be of help in refining our ideas as to the appropriate definition of the LME structure of the Indian Ocean off the coast of Africa. There are two major current systems off the African coast, the seasonally reversing Somali Current and the poleward Agulhas Current. Biologically, both would seem to be rather "leaky" systems, with the strongest enrichment occurring toward the downstream ends of particularly rapid advective "rides" (i.e., near the point where much of the resulting production exits the coastal system). This is not the ideal progression, in which movement would be from zones of enrichment toward zones of concentration and retention.

In such circumstances, areas of relative retention such as the Gulf of Aden and the Sofala Bight of Mozambique may deserve special consideration. The Gulf of Aden is well situated to be a retention zone, where enrichment from the Somali coastal upwelling could defuse into a less energetic environment in which concentration and retention processes could become effective. The Sofala Bight is more problematic with respect to enrichment by classic coastal upwelling, but there is no doubt that substantial primary production does occur (see Fig 6-9). These two zones, where endemic populations may be relatively maintainable on the long term, may serve as valuable sources of "seed stock" for the more dissipative segments of the regional ecosystems.

If so, the implication is that the Gulf of Aden may constitute a key component of the Somali Current LME system. Thus, consideration should be given to making it an integral part of any Somali Current LME management scheme. The situation of the Sofala Bight of Mozambique is more difficult to decide. The large-scale current pattern (see Fig 6-6) may influence one to view it more as a part of the southward flowing Agulhas Current LME system. However, seasonal reversals and gyre eddy patterns within the Mozambique Channel ensure that there is two-way communication also with the main Somali Current system, where its upstream location with respect to that uniquely powerful advective flow might make this coastal bight area a particularly valuable seed source for the downstream ecosystems. Additionally, the characteristic temperature range in the Sofala Bight is more comparable with that in the Somali system as a whole than to that in the Agulhas system where there exists a substantial downstream cooling tendency. It may therefore be useful, for conservation and management considerations, to think of the Sofala Bight, and in

fact the entire Mozambique Channel, as an integral component of the Somali Current LME.

References

1. Food and Agriculture Organization. Review of the state of the world fishery resources: marine fisheries. FAO Fish Circ 884, 1995.
2. Ardill JD, Sanders.MJ, eds. Proceedings of the Seminar to Identify Priorities for Fisheries Management and Development in the Southwest Indian Ocean, Albion, Mauritius, September 1991.
3. Sørensen NK, Beltestad A, Misund O. Trial fishing for anchovy 1985–1987. MOZ 037, Project review and conclusions. Institute of Fishery Technology Research, Tromsø, Norway.
4. Bakun A. Patterns in the ocean: ocean processes and marine population dynamics. San Diego, CA: University of California Sea Grant, in cooperation with Centro de Investigaciones Biológicas de Noroeste, La Paz, Baja California Sur, Mexico, 1996.
5. Rice J. Food web theory, marine food webs, and what climate change may do to northern marine fish populations. In: Beamish RJ, ed. Climate Change and Northern Fish Populations. Canadian Special Publication of Fisheries and Aquatic Sciences 121, 1995: 561–568.
6. Bakun A. The California Current, Benguela Current, and Southwestern Atlantic Shelf Ecosystems: a comparative approach to identifying factors regulating biomass yields. In: Sherman K, Alexander LM, Gold B, eds. Large Marine Ecosystems: Stress, Mitigation, and Sustainability. Washington, DC: AAAS, 1993:199–224.
7. Mayr E. The growth of biological thought. Cambridge, MA: Harvard Univ. Press, 1982.
8. Bakun A. Guinea Current upwelling. Nature 1978;271:147–150.
9. Bakun A, Parrish RH. Comparative studies of coastal pelagic fish reproductive habitats: the Brazilian sardine (*Sardinella aurita*). J Cons Int Explor Mer 1990;46:269–283.
10. Bakun A, Parrish RH. Comparative studies of coastal pelagic fish reproductive habitats: the anchovy (*Engraulis anchoita*) of the southwestern Atlantic. ICES J Mar Sci 1991;48: 343-361.
11. Bakun A, McLain DR, Mayo F. The mean annual cycle of coastal upwelling off western North America as observed from surface measurements. Fish Bull US 1974;72:843–844.
12. Parrish RH, Nelson CS, Bakun A. Transport mechanisms and reproductive success of fishes in the California Current. Biol Oceanogr 1981;1:175–203.
13. Wooster WS, Bakun A, McLain DR. The seasonal upwelling cycle along the eastern boundary of the North Atlantic. J Mar Res 1976;34:131–141.
14. Woodruff SD, Slutz RJ, Jenne RL, Steureer PM. A comprehensive ocean-atmosphere data set. Bull Am Meteor Soc 1987;68:1239–1250.
15. Roy C, Mendelssohn R. The development and the use of a climatic database for CEOS using the COADS dataset. In: Durand M-H, Cury P, Mendelssohn R, et al, eds. Global versus local changes in upwelling systems. Paris: ORSTOM editions (in press).
16. Wooster WS, Reid JL. Eastern boundary currents. In: Hill MN, ed. The sea, Vol. 2. New York: Interscience Pub., 1963:253–280.

17. Cushing DH. Upwelling and fish production. FAO Fish Technical Paper 84, 1969.
18. Hastenrath S, Lamb PJ. Climatic atlas of the Indian Ocean, part 1. Madison: University of Wisconsin Press, 97 charts, 1979.
19. Wooster WS, Schaefer MB, Robinson MK. Atlas of the Arabian Sea for fishery oceanography. La Jolla Inst Mar Resour IMR Ref. 67-12, 1967.
20. Wyrtki K. Oceanographic Atlas of the International Indian Ocean Expedition. Washington, DC: National Science Foundation, 1971.
21. Ekman VW. On the influence of the earth's rotation on ocean currents. Ark Mat Astron Fys 1905;2:1–55.
22. Anonymous. U.S. Joint Ocean Global Flux Study, Arabian Sea Process Study. U.S. JGOFS Planning Report No. 13, 1991.
23. Smith RL. Upwelling. Oceanogr Mar Biol Annu Rev 1968;6:11–46.
24. NSF/NASA. Ocean color from space. (A folder of remote sensing imagery and text, prepared by the NSF/NASA U.S. Global Ocean Flux Study Office.) Woods Hole, MA: Woods Hole Oceanographic Institution, 1989.
25. Shah NM. Seasonal variation of phytoplankton pigments and some of the associated oceanographic parameters in the Laccadive sea off Cochin. In: Zeitzschel B, ed. Biology of the Indian Ocean. London: Chapman and Hall, 1973:175–185.
26. Longhurst AR, Wooster WS. Abundance of oil sardine (*Sardinella longiceps*) and upwelling on the southwest coast of India. Can J Fish Aquat Sci 1990; 47:2407–2419.
27. Banse K. On upwelling and bottom-trawling off the southwest coast of India. J Mar Biol Assoc India 1959;1:33–49.
28. Mathew B. Studies on upwelling and sinking in the seas around India. Ph.D. thesis, University of Cochin, 1982.
29. McCreary JP Jr, Lee HS, Enfield DB. The response of the coastal ocean to strong offshore winds: with application to circulations in the Gulfs of Tehuantepec and Papagayo. J Mar Res 1989;47:81–109.
30. Roden GI. On the wind-driven circulation in the Gulf of Tehuantepec and its effect on surface temperatures. Geofis Int 1961;1:55–72.
31. Parrish RH, Bakun A, Husby DM, Nelson CS. Comparative climatology of selected environmental processes in relation to eastern boundary current pelagic fish reproduction. In: Sharp GD, Csirke J, eds. Proceedings of the Expert Consultation to Examine Changes in Abundance and Species Composition of Neritic Fish Resources. FAO Fish Rep 1983:731–778.
32. Hsueh Y, O'Brien JJ. Steady coastal upwelling induced by an along-shore current. J Phys Oceanogr 1971;1:180–186.
33. Paffenhöffer GA, Wester BT, Nicholas WD. Zooplankton abundance in relation to state and type of intrusions onto the southeastern United States shelf during summer. J Mar Res 1984;42:995–1017.
34. Dickson RR, Gurbutt PA, Pillai VN. Satellite evidence of enhanced upwelling along the European continental slope. J Phys Oceanogr 1980;10:813–819.
35. Mazé R, Camus Y, LeTareau JY. Formation de gradient thermiques à la surface de l'océan, au-dessuss d'un talus, par interaction entre les ondes et le mélange dû au vent. J Cons Int Explor Mer 1986;42:221–240.
36. Jury MR. A review of the meteorology of the eastern Agulhas Bank. S Afr J Sci 1994;90: 109–113.

37. Beckley LE. Sea-Surface temperature variability around Cape Recife, South Africa. S Afr J Sci 1982;79:436–438.
38. Shumann, EH, Perrins L-A, Hunter LT. Upwelling along the south coast of the Cape Province, South Africa. S Afr J Sci 1982;78:238–242.
39. Walker ND. Satellite observations of the Agulhas Current and episodic upwelling south of Africa. Deep-Sea Res 1986;33:1083–1106.
40. Schumann EH, Ross GBJ, Goshen WS. Cold water events in Algoa Bay and along the Cape south coast, South Africa in March/April 1987. S Afr J Sci 1988;84:579–584.
41. Boyd AJ, Shillington FA. Physical forcing and circulation patterns on Agulhas Bank. S Afr J Sci 1994;90:114–122.
42. Goshen WS, Schumann EH. Upwelling and the occurrence of cold water around Cape Recife, Algoa Bay, South Africa. S Afr J Mar Sci 1995;16:57–67.
43. Legendre L, Demers S. Auxiliary energy, ergoclines and aquatic biological production. Natur Can (Rev Ecol Syst) 1985;112:5–14.
44. Lasker R. The relation between oceanographic conditions and larval anchovy food in the California Current: identification of the factors leading to recruitment failure. Rapp P-v Réun Cons Int Explor Mer 1978;173:212–230.
45. Lasker R. Factors contributing to variable recruitment of the northern anchovy (*Engraulis mordax*) in the California Current: contrasting years 1975 through 1978. Rapp P-v Réun Cons Int Explor Mer 1981;178:375–388.
46. Lasker R. The role of a stable ocean in larval fish survival and subsequent recruitment. In: Lasker R, ed. Marine Fish Larvae: Morphology, Ecology and Relation to Fisheries. Seattle: Univ. Washington Press, 1981:80–87.
47. Peterman RM, Bradford MJ. Wind speed and mortality rate of a marine fish, the northern anchovy (*Engraulis mordax*). Science 1987;235:354–356.
48. Wroblewski JJ, Richmond JG. The non-linear response of plankton to wind-mixing events: implications for larval survival of northern anchovy. J Plankton Res 1987;9: 103–123.
49. Rothschild BJ, Osborn TR. The effects of turbulence on planktonic contact rates. J Plankton Res 1988;10:465–474.
50. Landry F, Miller TJ, Leggett WC. The effects of small-scale turbulence on the ingestion rate of flathead minnow (*Pimephales promelas*) larvae. Can J Fish Aquat Sci 1995;52: 1714–1719.
51. Sinclair M. Marine populations. An Essay on Population Regulation and Speciation. Washington Sea Grant Program. Seattle: Univ. Washington Press, 1988.
52. Bruce JG, Fieux M, Gonella J. A note on the continuance of the Somali eddy after the cessation of the Southwest Monsoon. Oceanol Acta 1981;4:7–9.
53. Swallow JC. Circulation in the Northwestern Indian Ocean. In U.S. Joint Ocean Global Flux Study, Arabian Sea Process Study. U.S. JGOFS Planning Report No. 13, 1991:37–48.
54. Wyrtki K. Physical oceanography of the Indian Ocean. In: Zeitzschel B, ed. Biology of the Indian Ocean. London: Chapman and Hall, 1973:18–36.
55. Cury P, Roy C. Optimal environmental window and pelagic fish recruitment success in upwelling areas. Can J Fish Aquat Sci 1989;46:670–680.
56. Mendelssohn R, Cury P. Forecasting a fortnightly abundance index of the Ivorian coastal pelagic species and associated environmental conditions. Can J Fish Aquat Sci 1987;44:408–421.

57. Mendelssohn R, Mendo J. Exploratory analysis of anchoveta recruitment off Peru and related environmental series. The Peruvian Anchoveta and Its Upwelling Ecosystem: three decades of change. In: Pauly D, Tsukayama I, eds. ICLARM Studies and Reviews 1987:294–306.
58. Cury P, Roy C, Mendelssohn R, et al. Moderate is better: nonlinear climatic effect on California anchovy. In: Beamish RJ, ed. Climate Change and Northern Fish Populations. Canadian Special Publication of Fisheries and Aquatic Sciences 1995;121:417–424.
59. Ware DM, Thomson RE. Link between long-term variability in upwelling and fish production in the northeast Pacific Ocean. Can J Fish Aquat Sci 1991;48:2296–2306.
60. Steele, JH. 1974. The Structure of Marine Ecosystems. Cambridge, MA: Harvard Univ. Press, 1988.
61. Sverdrup HU. On conditions for vernal blooming of phytoplankton. J Cons Int Explor Mer 1953;18:287–295.
62. Roy C, Cury P, Kifani S. Pelagic fish reproductive success and reproductive strategy in upwelling areas: environmental compromises. S Afr J Mar Sci 1992;12:135–146.
63. Elsberry RL, Garwood RW Jr. Sea-surface temperature anomaly generation in relation to atmospheric storms. Bull Am Meteorol Soc 1978;59:786–789.
64. Husby DM, Nelson CS. Turbulence and vertical stability in the California Current. CALCOFI Rep 1982;23:113–129.
65. Saccardo SA. Biología y disponibilidad de sardina (*Sardinella Brasiliensis*, Steindachneer, 1879) en la costa sudeste del Brazil. In: Sharp GD, Csirke J, eds. Proceedings of the Expert Consultation to Examine Changes in Abundance and Species Composition of Neritic Fish Resources. FAO Fish Rep. 1983:449–464.
66. Sharp GD. Areas of potentially successful exploitation of tunas in the Indian Ocean with emphasis on surface methods. Indian Ocean Programme Development Report No. 47. Rome: FAO, 1979.
67. Laurs RM, Lynn RJ. Seasonal migration of North Pacific albacore, *Thunnus alalunga*, into North American coastal waters: distribution, relative abundance, and association with Transition Zone waters. Fish Bull US 1977;75:795–822.
68. Pauly D. The relationships between gill surface area and growth performance in fish: a generalization of von Bertalanffy's theory of growth. Meeresforsch 1981;28:251–282.

Large Marine Ecosystems of the Indian Ocean: Assessment, Sustainability, and Management

:dited by

(enneth Sherman

)irector, Narragansett Laboratory; Chief, Oceanography Branch, Northeast Fisheries Science Center, National Marine Fisheries Service, Jational Oceanic and Atmospheric Administration; Adjunct Professor of)ceanography, Graduate School of Oceanography, University of Rhode sland, Narragansett, Rhode Island

:zekiel N. Okemwa

)irector, Kenya Marine and Fisheries Research Institute, Mombasa, Kenya

Aicheni J. Ntiba

'rofessor, University of Nairobi, Department of Zoology, Nairobi, Kenya; :xecutive Secretary, Lake Victoria Fisheries Organization (LFVO), Jinga, Uganda

b

lackwell Science

Contents